Design of the UWE-4 Picosatellite Orbit Control System using Vacuum-Arc-Thrusters

IEPC-2013-195

Presented at the 33rd International Electric Propulsion Conference,
The George Washington University, Washington, D.C., USA
October 6–10, 2013

Igal Kronhaus*, Klaus Schilling†, Satish Jayakumar ‡ *and* Alexander Kramer §
Department of Computer Science VII, Wuerzburg University, Wuerzburg 97074, Germany

Mathias Pietzka¶ *and* Jochen Schein‖
University of the Federal Armed Forces, Werner-Heisenberg-Weg 39, Neubiberg 85577, Germany

Abstract: An orbit control system has been designed for 1U CubeSats capable of maintaining spacecraft formation after deployment from a common launcher. This system is implemented in the UWE-4 CubeSat. Four thrusters are placed on one side of the CubeSat frame to achieve both two axis attitude control and orbit control. The propulsion system is based on vacuum-arc-thrusters. Thruster scalability allows to miniaturize and integrate it with the spacecraft structure. The small size of the power processing unit with volume and mass of less than 130 cm^3 and 150 g respectively is made possible due to the low voltage operation (25 V) and the simplicity of the ignition process. A legacy spacecraft bus with a proven attitude determination system is used with minimal modifications. Measurements of the ion current using multiple probes show that the thrust is directed, with a plume half angle of $\approx$ 45 deg. Time averaged thrust to power ratio is approximately 1.5 μN/W.

I. Introduction

CONSIDERABLE attention is given in the last years to the problem of lowering cost and time associated with the development of Earth observation and communication satellites, both for military and civilian uses.[1,2] One possible method of addressing these needs is by replacing a single large spacecraft with a distributed system of small satellites.[3,4] Several missions are currently being designed and flown to advance the state of the art in formation flying technology (for example PROBA-3 and PRISMA missions), taking advantage of the trend in spacecraft miniaturization.

On the low cost scale, several university programs are in progress to incorporate scientific payload and propulsion on CubeSats.[5] CubeSats are miniaturized modular satellites constructed as standardized units with corresponding launch adapters.[6] CubeSats vary in size from 1U to 12U where each unit (U) has a volume of $10 \times 10 \times 10$ cm^3 and mass of $\sim$ 1 kg. Currently, CubeSat formation flying experiments are being planned by several university groups.[7,8] Most utilize 2U and larger configurations in order to use

* Postdoctoral Fellow, Department of Computer Science VII, kronhaus@informatik.uni-wuerzburg.de, igalkron@gmail.com.
† Chair, Department of Computer Science VII, schi@informatik.uni-wuerzburg.de.
‡ Student, Department of Computer Science VII.
§ Student, Department of Computer Science VII.
¶ Research Associate, Institute for Plasma Technology and Mathematics (EIT 1), mathias.pietzka@unibw.de.
‖ Professor, Institute for Plasma Technology and Mathematics (EIT 1), jochen.schein@unibw.de.

conventional satellite technologies in miniaturized form.[9] Further reduction in size requires a significant change in spacecraft design and a higher integration between components.

An active research and development effort in this field is being carried out at Wuerzburg University. A series of picosatellites are being developed that conform to the 1U CubeSat standard. The first, UWE-1, launched in 2005. The UWE (University Wuerzburg Experimental) satellite program is intended to demonstrate enabling technologies for cooperating distributed small satellites, with the eventual goal of realizing such a system in space. The UWE-4 picosatellite is the first in the series to incorporate a propulsion system.

The necessary propulsion capabilities for UWE-4 are derived from a practical requirement to keep CubeSats at a bounded distance after deployment from a common launcher. The satellites need to be within line of sight with each other and a ground location. A circular orbit is considered at altitudes above 500 km where the drag force becomes negligible compared to other perturbations. Most CubeSat launches are made to similar orbits.

Analysis shows[10] that the most important factor determining the relative drift rate between the satellites, above altitudes of 500 km, is the differential semi-major-axis (SMA). Differences in SMA as large as 2 km were detected in real deployment scenarios. Accordingly, rates of change in relative distance of above 200 km/day were measured. Thus, without propulsion, a formation mission can be terminated in less than a month.

This paper focuses on the design of the UWE-4 CubeSat orbit control system. The paper is organized as follows: section II describes the mission scenario and the orbit/attitude control strategy; section III presents the satellite bus including hardware and main functions; section IV describes in detail the vacuum-arc-thruster propulsion system and section V presents the thruster test system and initial results.

II. Orbit Control with Limited Power and Orbit Determination Accuracy

Picosatellites have strict power limitation. 1U CubeSat, without deployable solar arrays, can generate an average power of 1.5 - 2.5 W. The power restriction affect an orbit control system, equipped with electric propulsion, in two important ways: (1) electric propulsion systems are limited to thrust levels of few μN; (2) the power requirement of an on-line orbit determination systems is ≥ 1 W,[11] too high when combined with an electric propulsion system.

To address these restrictions an off-line ground based orbit control system was developed in Ref. 10, utilizing several two-line elements (TLE) data sets and an on-board switching control. A controller is chosen with a time constant of few days, allowing for several TLEs to be acquired, thus improving the orbit determination accuracy. The relative distance between a pair of satellites $\boldsymbol{\rho} = \boldsymbol{r}_i - \boldsymbol{r}_0$ (the chief satellite is indexed 0) is defined in the local-vertical local-horizontal (LVLH) frame as shown in Fig. 1. The considered basic formation requires to keep the $\rho < 1500$ km (about half the line of sight distance to a point on the ground) throughout the mission duration of several months.

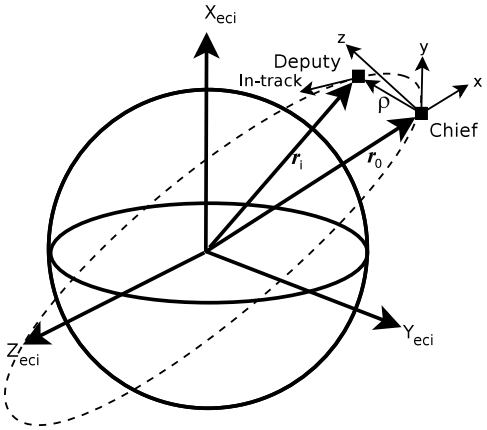

Fig. 1: Local-vertical local-horizontal (LVLH) reference frame definition.

A simple bang-bang control is used. If the deputy satellite has drifted behind the chief, it applies

acceleration in the anti-in-track direction in order to decrease its SMA and hence increase its velocity in the in-tack direction. Once past the chief satellite, the deputy applies positive acceleration to increase its SMA and slow itself with respect to the chief. The control law requires only to determine the points of closest approach, when the satellites move past each other, and then to apply the following command change:

$$\boldsymbol{u} = \begin{cases} u_{max}\hat{\boldsymbol{u}}_{\text{in-track}} & \text{if} \quad y \geq 0 \\ -u_{max}\hat{\boldsymbol{u}}_{\text{in-track}} & \text{if} \quad y < 0, \end{cases} \tag{1}$$

where u_{max} is the maximum spacecraft acceleration and y is the in-track position of the deputy relative to the chief. High fidelity simulations of this control law show that a bounded formation of 1500 km can be maintained with an average ΔV of 2.5 m/s per month. A continues average thrust of 1 μN was modeled.

In the suggested simple orbit controller the thrust vector has to be aligned either with the in-track or anti-in-track direction, this implies that the spacecraft has to be turned according to its orbital position. Due to power restrictions the use of reaction wheels during application of thrust is not possible, as the smallest types require at least 0.5 W per wheel.[12] Instead, thrusters can be used to create the necessary torques. Using four thrusters positioned on one side of the CubeSat frame, a two axis attitude control can be achieved. The rotation around the in-track direction is left uncontrolled. Following the simple orbit controller maximum thrust has to be applied continuously, thus a bang-bang control is considered for attitude control.[13] Due to the above mentioned power restrictions only one thruster can operate at full thrust at a given time.

To summarize, a combined attitude and orbit control scheme is considered where the attitude correction is automatically controlled on-board the satellite, whereas the orbit control commands are updated once every few days from the ground.

III. UWE-4 Spacecraft Bus and Orbit Control System

As previously discussed the UWE-4 pico-satellite is an in-track pointing two-axis stabilized 1U CubeSat. The satellite frame is composed of four parallel rails separated 10 cm from each other and solar panels in between. Separation springs and kill switches are accommodated inside the rail ends on the bottom side to ensure and indicate proper separation from the launch adapter. Four vacuum-arc-thrusters are mounted on the top side of the rails. The outer structure is decoupled from the electronics inner structure, as shown in Fig. 2. The major subsystems are described in Table 1.

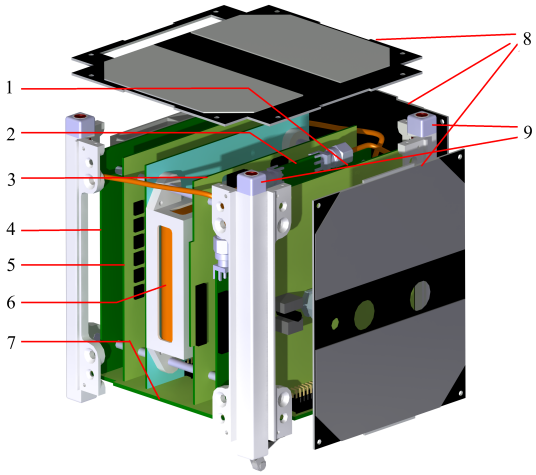

Fig. 2: Structural overview of the UWE-4 1U CubeSat: (1) front access board, (2) PPU, (3) attitude determination and control, (4) communication, (5) on-board data handling, (6) power system, (7) backplane, (8) panels, and thrusters (9).

The UWE-4 mission is to demonstrate the capability of a picosatellite to perform useful orbital maneuvers. A first requirement is to have sufficiently accurate determination of the attitude and orbital position of the spacecraft. The attitude determination of UWE-4 is based on measuring the local magnetic field vector and

Table 1: UWE-4 main systems.

Attitude and Orbit Control 2-axis stabilized; $<$ 5 deg attitude accuracy; $<$ 1 deg control pointing accuracy; SGP4 orbit propagator with two-line elements update 1-2 km accuracy; off-line orbit control	**Communications** 2 redundant UHF radios; maximum downlink/uplink data rates are 9.6 kbit/s
Power triple junction GaAs solar cells with 28 % efficiency; maximum power of 4 W (2.5 W orbit average); 2 Li-ion batteries 2.6 A-h each; 3.7 - 4.2 V DC	**Propulsion** four vacuum-arc-thrusters; few grams of propellant provides $\Delta V \leq 10$ m/s for formation flying maneuvers
On-board Data Handling 2 redundant MSP430 1MHz Processors; 16 kB RAM and 8 Mb of flash memory; I2C bus	**Thermal** passive; battery housing is decoupled from the external surfaces and includes heaters

the sun vector. The available sensors and actuators are listed in Table 2. An isotropic Kalman Filter (IKF) performs the attitude state prediction and sensor fusion. The IKF compares the measured vectors to the model magnetic field and the model sun reference. A simplified perturbations model 4 (SGP4) is used to calculate the orbital position. The SGP4 propagator is regularly updated from the ground station when a new TLE is available.

The hardware architecture of the orbit and attitude control system is provided in Fig. 3. The attitude determination and control system (ADCS) computer calculates the attitude estimation from on-board rate gyroscopes and magnetometers. The sun vector is obtained from sun sensors installed on each of the six panels. This is a proven system developed for the previous UWE-3 picosatellite.[14]

The attitude is controlled by a combined use of magnetorquers and thrusters. An air coil magnetorquer is mounted on each panel. Their primary function is to detumble the satellite i.e., to slow down its initial rotation after ejection from the deployer. The magnetorquer control law is independently computed on each panel according to the angular rate data sent from the ADCS.

The thruster control is activated once the rate of rotation is reduced below 1 deg/s. A microcontroller on the power processing unit (PPU) receives the current S/C attitude, target attitude, angular velocity, and the time window given for operation from the ADCS. According to the attitude control law and the given time, the PPU selects the thruster to be fired and then generates the pulse width modulated (PWM) signal to the respective thruster head. The thruster attitude control law, described in Ref. 13, is capable of providing fine two-axis attitude pointing. Considering a control thrust magnitude of 2 μN and 1U CubeSat parameters, high fidelity simulations results show that an attitude accuracy of 0.5 deg can be maintained. In addition, the magnetorquers can augment the thrusters by providing control over the rotation rate in the third axis - along the thrust vector.

Limited orbit control is achieved by thrusting in the in-track or anti-in-track directions. The thrusters are constantly being fired (one at a time) to keep a modest acceleration of few 10^{-6} m/s. The thrust direction in Eq. (1) is sent from the ground station. The on-board data handling system transfers the command to the ADCS. Consequently the ADCS modifies the required target attitude to be transferred to the PPU.

IV. UWE-4 Propulsion System Spacecraft Integration

IV.A. Vacuum-Arc-Thruster

Volume, mass, and power constraints in picosatellites require the use of innovative propulsion solutions. For example, UWE-4 generates approximately 2.5 W of continues power of which about 2 W is available to the propulsion system. Only handful state-of-the-art propulsion systems are currently suitable[15] for this power

Table 2: UWE-4 sensors and actuators.

Component	Description
Magnetometer	3 perpendicularly mounted single axis magnetometers, 6 additional mounted one per panel; typical accuracy $< 2\mu$T
Sun sensor	6 sensors, one per panel; typical accuracy < 5 deg
Rate Gyro	3 perpendicularly mounted single axis rate gyros; typical accuracy 0.2 deg/s; max angular rate ± 320 deg/s
Magnetorquer	6 air coils, one per panel; max magnetic dipole strength ± 0.028 Am^2
Vacuum-Arc-Thruster	4 VATs are mounted on the tips of the rails; impulse bits of 0.01 - 0.1 μNs at freq. up to 20 Hz; arm length of 0.05 m for each axis

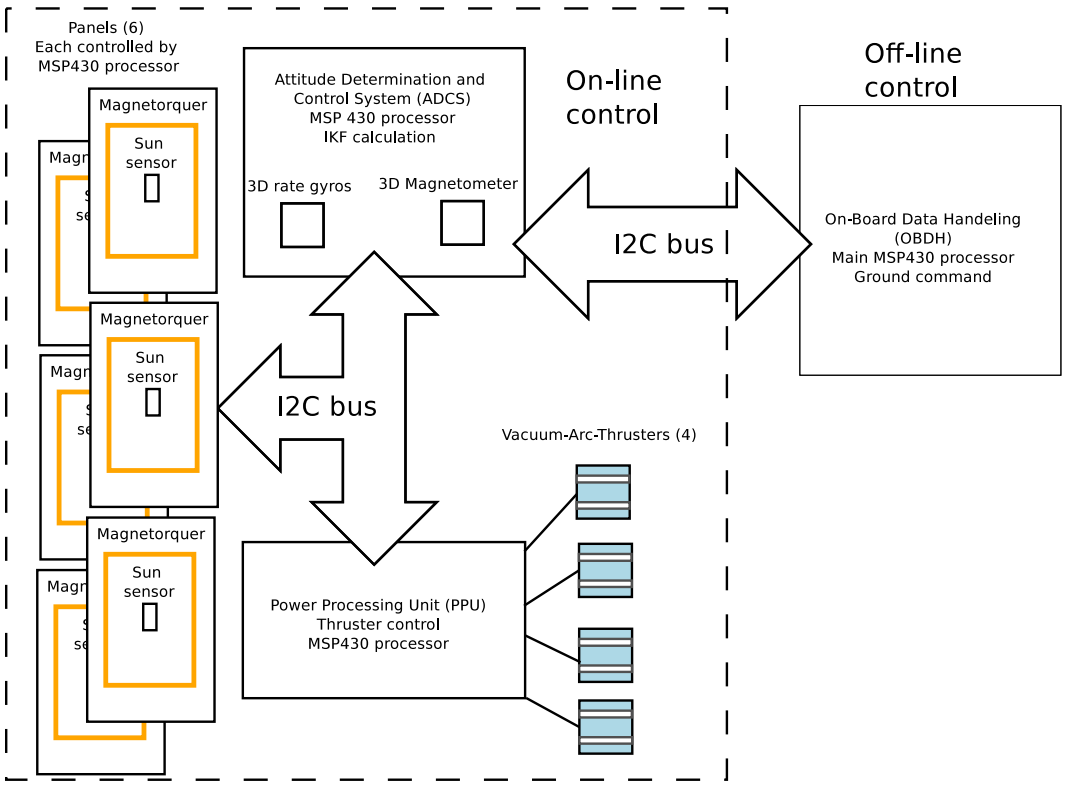

Fig. 3: Hardware architecture of UWE-4 orbit and attitude control system.

level. Among the few the vacuum arc thruster (VAT), an electric propulsion device, is a promising candidate. This type of thruster is simple, scalable, and has adequate performance in very low power operation.[16] The University of the Federal Armed Forces in Munich (UniBwM) together with Wuerzburg University develop

the micro-VAT for the UWE-4 picosatellite. The propulsion system is composed of two parts: thruster heads and the PPU.

UWE-4 uses a proven modular bus that was developed in Wuerzburg University.[17] The PPU is integrated as standard subsystem in the bus whereas the thrusters are accommodated on the outer structure rails. This arrangement is advantageous from several respects: (1) reduces plume contamination on the solar panels; (2) reduces the propulsion system volume and mass; (3) provides higher torques; (4) enables flexibility in PPU placement.

The VAT operates when high enough voltage is applied between the anode and cathode to form an arc discharge, as shown schematically in Fig. 4. The discharge is sustained by attaching to the cathode in localized areas, less than 10 μm in diameter, known as cathode spots. Each spot can produce up to hundred amperes by field enhanced thermionic emission.[18] Spot lifetime is < 0.1 μs. Once extinguished another spot is created that leads to an apparent random movement of the cathode spot across the cathode surface. The spot emits electrons and material vapor by explosive emission into the inter-electrode gap.[19] The vapor is fully ionized and the resulting plasma conducts the electron current between cathode and anode. Thrust is created by fast ions that carry about 10 % of the current. The ionized plasma is accelerated by supersonic flow expansion to velocities of $\sim 10^4$ m/s.[20]

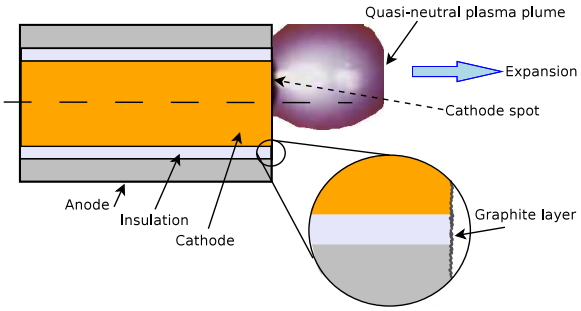

Fig. 4: Vacuum arc thruster operation principles.

The ion flow is mainly directed away from the cathode surface following a cosine distribution.[21] The selection of cathode material is important as it affects the ion current fraction α_i, the ion velocity V_i, the ion charge state $< Z >$, and the cathode erosion rate γ_c. It is important to note that the cathode erosion rate is a combination of both vapor mass and macro-particle mass. The macro-particles are charge neutral and are not accelerated to high velocities, thus they do not contribute to the thrust. Table 3 summarizes the effect of cathode material on these parameters.

Table 3: Ion fraction, ion velocities, ion average charge state, and erosion rates for different cathode materials. Taken from published data in Refs. 21, 22.

Cathode material	α_i, %	$< V_i >$, km/s	$< Z >$	γ_c, μg/C
Sn	11.4	1.37	1.52	80
Al	11.2	5.93	1.72	28
Cu	11.4	7.79	2.04	35
W	5.0	10.58	3.125	55

An important advance has enabled the miniaturization of the VAT - the so called triggerless operation.[22] By coating the inter-electrode dielectric gap with a thin conducting film (usually a carbon layer) with finite resistance, relatively low voltages of few hundred volts are required to ignite the discharge. The triggerless thruster was operated successfully for more than several 10^5 pulses at low pulse energy ~ 100 mJ.

The VAT thrust to power ratio is between 1 - 10 μN/W. With a fixed cathode the VAT has an expected total impulse of few Ns, which corresponds to $\Delta V \leq 10$ m/s for a 1 kg picosatellite. The total impulse can be extended with the use of a feeding mechanism to replenish the eroded cathode material. To accomplish a velocity change of $\Delta V = 7.5$ m/s as derived from the mission analysis,[10] approximately 1 g of propellant mass is needed (split between four thrusters) assuming a tungsten cathode with Isp ≈ 1000 s.

IV.B. Power Processing Unit Hardware

An efficient power processing unit is necessary to condition the voltage and current produced by the photovoltaic cells (≈ 4 V and 0.5 A respectively) to the required VAT pulse operation, with voltage of 20 - 30 V and current above 10 A.

The PPU electronics are mounted on a single standardized subsystem module. The PPU is comprised of a DC/DC converter that rises the bus voltage to 25 V and four separate switched inductive energy storage systems.[23] Every thruster has a dedicated transformer to store energy and isolate the primary coil from the secondary coil (thruster). This allows to protect the power electronics from the high voltages produced during the ignition process. Moreover, it allows to maintain the cathode and the external surfaces at the same potential and to avoid ground loops. The discharge current, the capacitor current, and the capacitor voltage are measured by the microcontroller analog to digital converter (DAC). The PPU electrical schematic is shown in Fig. 5.

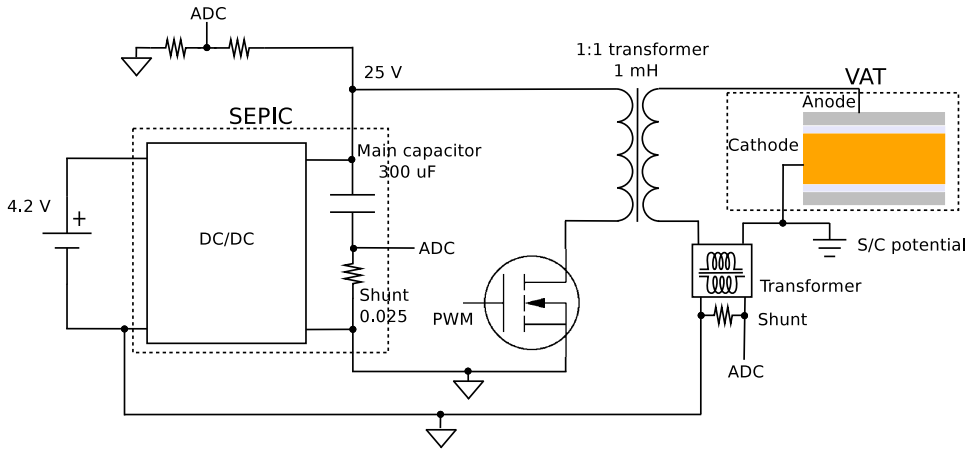

Fig. 5: Schematics of the PPU (only one thruster is shown). Microcontroller interfaces are emphasized (ADC and PWM).

The DC/DC converter's capacitor buffers the bus power supply from the relatively high current used during the thrust pulse. The primary inductor is charged from the capacitor. Once the metal-oxide-semiconductor field-effect transistor (MOSFET) is disconnected the current is discharged through the secondary coil and the VAT. At the moment the switch is opened a voltage peak of LdI/dt is created that breaks down the thin coating between anode and cathode.

The PPU is designed to generate pulse energies between 10 mJ and few 100 mJ with a pulse frequency of 1 – 20 Hz. The PPU total mass is ≈ 150 g and the total propulsion system mass is 200 g. The pulse energy and frequency are digitally controlled. The PPU also provides for fault protection and is tasked with sampling the discharge current and voltage. During the mission it is planned that the PPU data will be stored on the S/C computer and then transmitted to the ground station for analysis.

IV.C. PPU Functions and Telemetry

Four different time constants affect thruster operations: every 1 s the attitude data is updated; the SEPIC capacitor charge time is 60 - 100 ms; the primary coil charge time is 1 ms and the thruster discharge time is of few 100 μs (through the secondary coil).

The ADCS information is used by the PPU microcontroller to calculate which thruster will fire according to the attitude control algorithm.[13] The total number of pulses is set by the allowed time duration for PPU operation. The torque control is performed by the following sequence: (1) every 1 s the PPU receives the S/C attitude, the target attitude, the angular velocity with respect to reference frame, and the time available for thrust execution; (2) the PPU calculates which thruster has to fire and the number of pulses to be fired; (3) a PWM pattern is generated, switching the respective MOSFET to charge and discharge the primary coil.

The PWM waveform is shown in Fig. 6. It is composed from a raising edge event that closes the

MOSFET switch and starts to charge of the corresponding transformer's primary coil. At a preset delay, when the coil is fully charged, the falling edge triggers open the MOSFET. As a results, current is induced in the secondary coil and through the thruster.

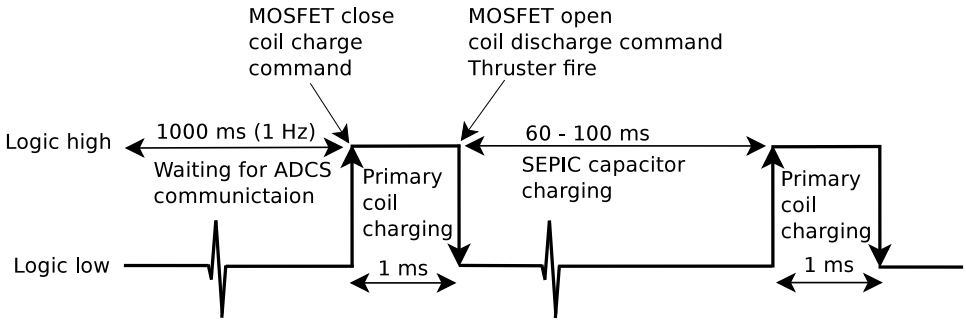

Fig. 6: PWM command timing sequence.

During operation the PPU microcontroller samples the secondary coil current every 50 μs as well as the capacitor voltage (every 1 ms) and the capacitor current (50 μs). The time duration of the discharge current through the thruster is recorded as well, by a use of a comparator. To a first approximation the generated impulse is linearly dependent on the pulse width time. The PPU output and telemetry functions are presented in Table 4.

In the closed-loop operation the microcontroller logic generates a PWM signal according to the sampled capacitor voltage, thus improving the propulsion system efficiency and firing rate. This allows to detect misfires and repeat the process until all the required pulses were generated.

Table 4: PPU output and telemetry.

PPU Output
PWM MOSFET 1
PWM MOSFET 2
PWM MOSFET 3
PWM MOSFET 4
PPU Telemetry on Serial Comm.
Receive S/C attitude, angular velocity, and target attitude
Send SEPIC capacitor voltage
Send SEPIC discharge current
Send thruster discharge current
Send thruster discharge current time duration
Send SEPIC capacitor temperature

V. Hardware Testing

A specially designed test stand was built in Wuerzburg University to measure the plume properties of the thrusters. The main goal is to determine the spatial distribution of the ion current density. This allows to calculate the total ion current and to establish the deviation of the plume vector (or thrust vector) from the vertical. This information is then used to calibrate the control system.

The propulsion system test stand is housed in a 100 l vacuum chamber equipped with a 16 m^3/h rotary vane pump and 330 l/s turbo pump. Pressure during measurements is 10^{-4} mbar. The test stand, schematically shown in Fig. 7, is comprised of four elements: (1) a satellite engineering model equipped with a PPU and four thrusters; (2) 16 planar probes located on a hemispheric structure with a radius of 0.12 m, the probes are connected to a switching system that multiplexes the probe signals to a single output wire;

(3) an isolated DC power supply is used to bias the probes to -70 V, located outside of the chamber; (4) A 100 Ohm resistor shunt converts the ion current to a voltage measured by a digital oscilloscope. The satellite, multiplexer and oscilloscope are remotely controlled from a PC running MATLAB. This setup allows to automatically measure the ion current distribution while validating the PPU operation and telemetry. Currently, as the PPU is only partially assembled, tests were performed using an external PPU with the discharge current measured using a Pearson coil. A typical measurement of the discharge current and the ion current during one pulse is shown in Fig. 8.

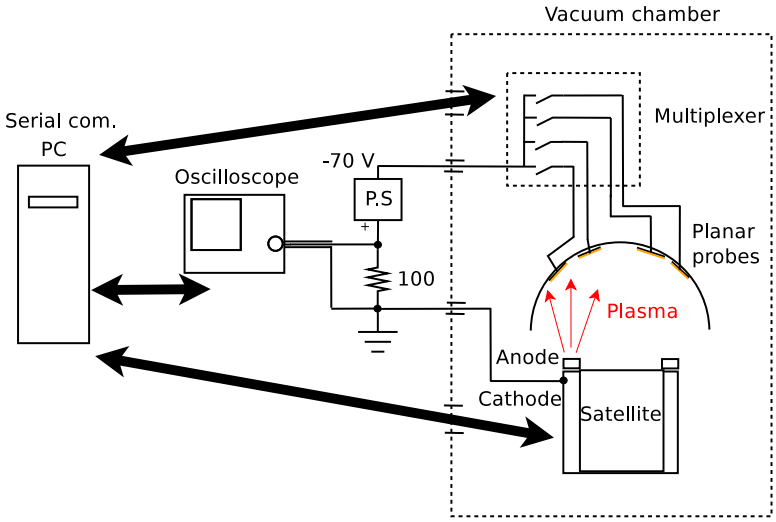

Fig. 7: Electrical schematic of the propulsion system test stand in Wuerzburg University.

The test procedure is as follows. The oscilloscope is prepared to trigger and the measurement geometry is selected by the multiplexer. Next, the PC sends a command to the PPU and the PPU fires one of the thrusters once. The ion current (and the discharge current when an external PPU is used) is captured by the oscilloscope. This data is then automatically downloaded to the PC. The PPU transmits back the diagnostics information including the discharge current and the capacitor voltage. Each probe measurement is repeated 10 times and the process continues until a spherical cap with a half angle of ≈ 60 deg is obtained.

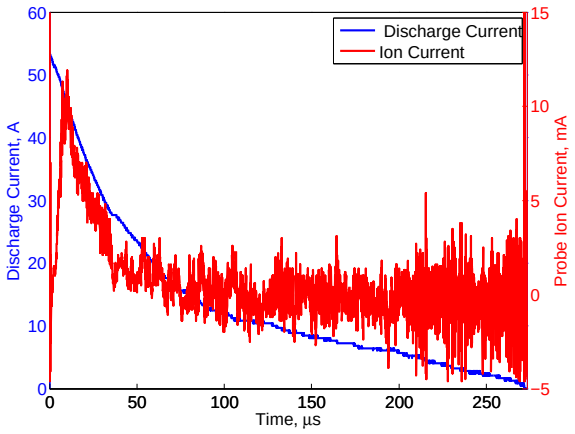

Fig. 8: Typical measurement result of the discharge current and probe ion current (Cu cathode, 150 mJ pulse).

In order to evaluate the spatial distribution of the ion current density, the maximum ion current value is compared between different probes. For each probe, the peak ion current is found by averaging over at least 10 different firings. The local ion current density is simply calculated by dividing the current by the probe area (10^{-4} m^2). As the peak discharge current varied less than 2 % between firings the data collection is

considered reliable. Moreover, the average result is of importance since the thrust is created by four thrusters during many activations.

By assembling 160 probe measurements a composite image of the ion current density is created, visualized by the use of a spherical coordinate system. An example result for a Cu cathode is shown in Fig. 9, where half the ion current (or thrust) is contained within a spherical cap ≈ 45 deg half angle. The total integrated ion current in this case is $I_{ion} \approx 2.82$ A. The ion velocity, estimated from the time difference between peak discharge and peak ion currents is $V_i \sim 11500$ m/s. The impulse is then calculated as:

$$T = \frac{MI_{ion}}{e<Z>} V_i \Delta t_p, \tag{2}$$

where Δt_p is the measured effective pulse duration, $M = 1.054 \times 10^{-25}$ kg is the Cu ion mass, and e is the electron charge. With a known charge state of 2, measured $\Delta t_p \sim 20$ μs, and a PPU efficiency of 90 % the impulse to input power P in this case is $T/P \sim 1.5$ μNs/W.

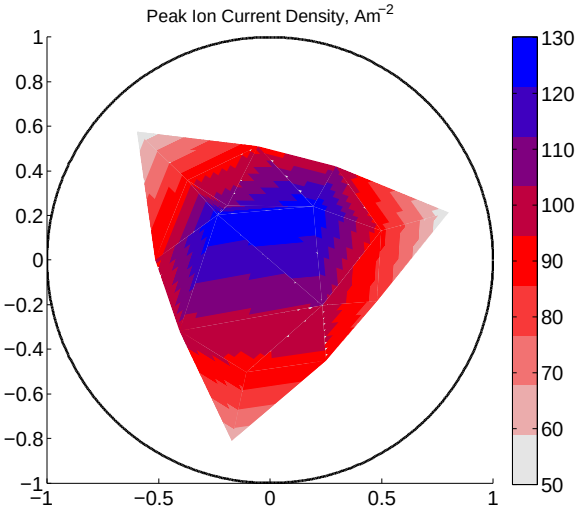

Fig. 9: Ion current density distribution measured by biased planar probes positioned on a spherical cap of 60 deg half angle and 0.118 m radius. The thruster (with a Cu cathode) is located at the center of the plot. The black circle represents a unit sphere.

VI. Conclusion

The UWE-4 1U CubeSat has been designed to demonstrate limited orbit control for maintaining a CubeSat formation. A vacuum-arc-thruster propulsion system was selected with a target $\Delta V \approx 10$ m/s and thrust values of 1 - 2 μN. The scalability and simplify of the vacuum-arc-thrusters, with no moving parts and a solid propellant, enable to integrate them with the structure of the spacecraft. The ignition process of the thrusters requires relatively simple power electronics and software procedure. The low power and voltage operation allow to use standard low mass commercial components. The spacecraft modular bus together with the integrated thrusters and miniaturized PPU enable to incorporate a propulsion system in a 1U CubeSat with little change to the rest of the satellite systems, retaining much of the proven design. Using multiple biased probes and hundreds of discharge measurements, it was found that the plume is roughly symmetrical with a half angle of ≈ 45 deg. For a Cu cathode, ion velocities above 10^4 m/s were measured with a calculated time-averaged thrust-to-power ratio of 1.5 μN/W, sufficient for the intended attitude control and orbit control applications.

Acknowledgments

Support for this research was provided by the Bavarian Space Technology Program from the project "Innovative propulsion system for satellite formations based on vacuum arc thrusters". I. K. gratefully

acknowledges the Minerva Foundation for the financial support. The authors wish to acknowledge Dieter Ziegler and Stephan Busch (Wuerzburg University) for their support with the CubeSat hardware.

References

[1]Richards, M. G., Viscito, L., Ross A. M., and Hastings D. E., "Distinguishing Attributes for the Operationally Responsive Space Paradigm," In Proceedings of 6th Responsive Space Conference, 2008, AIAA-RS6-2008-1004.

[2]Remuss, N. L., "Responsive Space for Europe," In ESPI Report, Vol. 22, 2010, ESPI European Space Policy Institute.

[3]Schilling, K. and Schmidt., M., "Status and Issues Related to In-Space Propulsion Systems," in book *Distributed Space Missions for Earth System Monitoring* edited by D'Errico, M., 2010, pp. 345 354, Springer, New York.

[4]Alfriend, K. T., Vadali, S. R., How, J. P., and Breger, L. S., *Spacecraft Formation Flying: Dynamics, Control and Navigation*, Elsevier Astrodynamics, 2010.

[5]Selva, D. and Krejci, D., "A Survey and Assessment of the Capabilities of Cubesats for Earth Observation," *Acta Astronautica*, Vol. 74, 2012, pp. 50–68.

[6]The CubeSat Program, "CubeSat Design Specifications (CDS) Rev. 12," California Polytechnic State Univ., San Luis Obispo, CA, 2009.

[7]"Formation Flying with in a Constellation of Nano-satellites: The QB50 Mission," *Acta Astronautica*, Vol. 82, 2013, pp. 110–117.

[8]Gurfil, P., Herscovitz, J., and Pariente, M., "The SAMSON Project - Cluster Flight and geolocation with Three Autonomus Nano-Satellites," In Proceedings of the 26th Annual AIAA/USU Conference on Small Satellites, 2012.

[9]Conversano, R. W. and Wirz, R. E., "Mission Capability Assessment of CubeSats Using a Miniature Ion Thruster," *Journal of Spacecraft and Rockets*, 2013, pp. accessed June 18, 2013. doi: 10.2514/1.A32435.

[10]Kronhaus, I., Pietzka, M., Schilling, K., and Schein, J., "Pico-satellite Orbit Control by Vacuum Arc Thrusters as Enabling Technology for Formation of Small Satellites," In Proceedings of the 5th International Conference on Spacecraft Formation Flying Missions and Technologies, Munich, May 29–31, 2013.

[11]Montenbruck, O., Gill, E., and Markgraf, M., "Phoenix-XNS–A Miniature Real-Time Navigation System for LEO Satellites," In Proceedings of NAVITEC'2006, 1–13 December, 2006.

[12]Stoltz, S., Driescher. H., and Kayal, H., "Development of the Micro Reaction Wheel RW 1," In Proceedings of the 7th International ESA Conference on Guidance, Navigation and Control Systems, Ireland, 2008.

[13]Kronhaus, I., Schilling, K., Pietzka, M., and Schein, J., "Simple Orbit and Attitude Control using Vacuum-Arc-Thrusters for Picosatellites," *Journal of Spacecraft and Rockets*, In review.

[14]Reichel, F., Bangert, P., Busch, S., Ravandoor, K., and Schilling, K., "The Attitude Determination and Control System of the Picosatellite UWE-3," In Proceedings of the 19th IFAC Symposium on Automatic Control in Aerospace, Wuerzburg, Germany, September 2–6, 2013.

[15]Mueller, J., Hofer, R., and Ziemer, J., "Survey of Propulsion Technologies Applicable to CubeSats," 57th Joint Army Navy NASA Air Force (JANNAF) Propulsion Meeting, Colorado Springs, CO, May 3-7, 2010. Available at JPL, Beacon eSpace, http://hdl.handle.net/2014/41627 (accessed 18 June 2013).

[16]Schein, J., Qi, N., Binder, R., and Krishnan, M., "Low Mass Vacuum Arc Thruster System for Station Keeping Missions," *Proceedings of the 27th International Electric Propulsion Conference*, IEPC paper 2001-228, 2001.

[17]Busch, S. and Schilling, K., "UWE-3: A Modular System Design for the Next Generation of Very Small Satellites," In Proceedings of Small Satellites Systems and Services - The 4S Symposium 2012, 2012.

[18]Juttner, B., "Cathode Spots of Electric Arcs," *J. Phys. D: Appl. Phys.*, Vol. 34, 2001, pp. 103–123.

[19]Mesyats, G. A., "Ecton Mechanism of the Vacuum Arc Cathode Spot," *IEEE Trans. on Plasma Sci.*, Vol. 23, No. 6, 1995, pp. 879–883.

[20]Beilis, I., "Theoretical Modeling of Cathode Spot Phenomena," in book *Handbook of Vacuum Arc Science and Technology Fundamentals and Applications* edited by Boxman, R. L., Sanders, D. M., and Martin, P. J., 1995, pp. 238–256, Noyes Publications, New Jersey.

[21]Polk, J. E., Sekerak, M. J., Ziemer, J. K., Schein J., Qi, N., and Anders, A., "Theoretical Analysis of Vacuum Arc Thruster and Vacuum Arc Ion Thruster Performance," *IEEE Trans. on Plasma Sci.*, Vol. 36, No. 5, 2008, pp. 2167–2179.

[22]Anders, A., Schein, J., and Qi, N., "Pulsed vacuum-arc ion source operated with a triggerless arc initiation method," *Review of Scientific Instruments*, Vol. 71, No. 2, 2000, pp. 827–829.

[23]Schein, J., Qi, N., Binder, R., Krishnan, M., Ziemer, J. K., Polk, J. E., and Anders, A., "Inductive Energy Storage Driven Vacuum Arc Thruster," *Review of Scientific Instruments*, Vol. 73, No. 2, 2002, pp. 925–927.